Earth and Planetary Science Letters 572 (2021) 117116

Contents lists available at ScienceDirect

Earth and Planetary Science Letters

www.elsevier.com/locate/epsl

Global continental volcanism controlled the evolution of the oceanic nickel reservoir

He Liu [a,b,c,*], Kurt O. Konhauser [d,*], Leslie J. Robbins [e], Wei-dong Sun [a,b,c]

[a] Center of Deep-Sea Research, Institute of Oceanology, Chinese Academy of Sciences, 7 Nanhai Road, Qingdao 266071, China
[b] Laboratory for Marine Mineral Resources, Qingdao National Laboratory for Marine Science and Technology, Qingdao 266237, China
[c] Center for Ocean Mega-Science, Chinese Academy of Sciences, 7 Nanhai Road, Qingdao 266071, China
[d] Department of Earth and Atmospheric Sciences, University of Alberta, Edmonton, Alberta T6G 2E3, Canada
[e] Department of Geology, University of Regina, Regina, Saskatchewan S4S 0A2, Canada

ARTICLE INFO

Article history:
Received 30 March 2021
Received in revised form 10 July 2021
Accepted 15 July 2021
Available online xxxx
Editor: F. Moynier

Dataset link:
https://github.com/Codrlocas/Nickel.git

Keywords:
volcanic rocks
Precambrian
nickel
shales
BIF

ABSTRACT

Wanning nickel (Ni) abundances in the Neoarchean may have led to a decline in marine methanogenic bacteria due to the loss of a key micronutrient, causing a collapse in atmospheric methane levels and the subsequent rise of atmospheric oxygen – the Great Oxidation Event ~2.5 Ga. However, this hypothesis currently lacks geological evidence that corroborates the processes that led to a decline in the supply of Ni to the oceans at that time. Here we investigate temporal variations of Ni concentrations in the likely source rocks – various volcanic lithologies - spanning the past 3.5 Byr. By applying a spatially gridded resampling to geochemical data from a global compilation of ~96,000 continental volcanic rocks, we show that komatiites and basaltic-andesitic rocks largely controlled Ni fluxes to the Earth's surface during the Archean but had a waning influence thereafter due to the secular cooling of the mantle. A new compilation of marine shales (397 samples) and an updated compilation of banded iron formations (2037 samples) further confirms a declining clastic and dissolved supply of terrestrial Ni, respectively. Interestingly, we further observed a stable marine Ni concentration for the last 2 Byr. To explain this unexpected trend, we provide a computational model of mantle melting demonstrating that increasing melting pressures likely inhibited a further decline of Ni concentration in volcanic rocks and led to this relative consistency in Ni supply.

1. Introduction

Abundant models for the composition of Earth's atmosphere prior to the Great Oxidation Event (GOE, ~2.5-2.1 Ga) (Lyons et al., 2014; Poulton et al., 2021) suggest that a relatively large amount of methane (CH_4) existed under the low-oxygen (O_2) conditions that persisted in the coupled atmosphere-ocean system (Canfield et al., 2000; Habicht et al., 2002; Haqq-Misra et al., 2008; Lyons et al., 2014; Pavlov et al., 2000). Based on the secular variation of molar Ni/Fe in banded iron formations (BIF), a decline in Ni abundance in the Archean ocean was identified (Konhauser et al., 2009, 2015). The decreased Ni concentrations in the ancient marine water column would have stifled methanogens and reduced the production of biogenic methane (Konhauser et al., 2009). A collapse in atmospheric methane might have facilitated the rise of atmospheric oxygen at the beginning of the Paleoproterozoic (Catling et al., 2001; Zahnle et al., 2006). Thus, the evolution of Ni abundance in the ancient ocean is crucial to understanding the transition from a CH_4-rich to an O_2-rich atmosphere.

The decline in dissolved Ni concentrations in Archean seawater was attributed to a reduced flux of volcanic Ni to the oceans, specifically the gradual decrease in komatiite eruptions (Greber et al., 2017; Konhauser et al., 2009, 2015). However, no detailed evidence for changing volcanic eruptions was provided, and thus it remains to be demonstrated whether a shift in Ni sourcing was indeed the reason for the observed temporal Ni variations in seawater through time. To address these critical uncertainties, this work focused on a statistical analysis of continental volcanic rock compositions throughout Earth's history. We applied a grid-resampling method to an extensive geochemical database and, for the first time ever, obtained the temporal variations of average Ni concentrations in all types of continental volcanic rocks. We also provide an updated database of Ni concentration in BIF and present a comparable shale record. Our collective database provides convincing evidence for the decrease in the bulk volcanic Ni supply to the oceans during the Neoarchean and early Paleoproterozoic, substan-

* Corresponding authors.
E-mail addresses: liuhe@qdio.ac.cn (H. Liu), kurtk@ualberta.ca (K.O. Konhauser).

https://doi.org/10.1016/j.epsl.2021.117116
0012-821X/

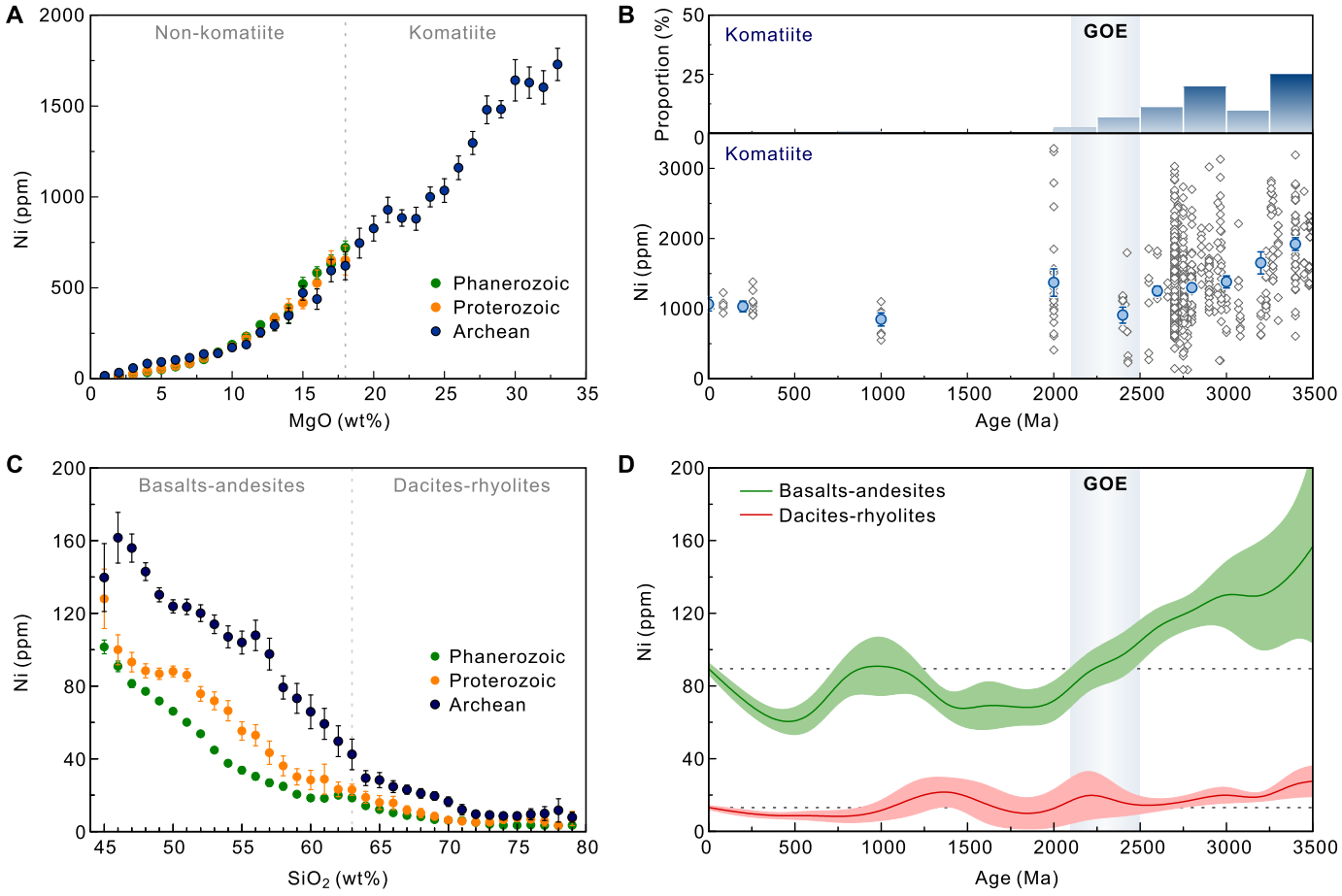

Fig. 1. Variations of Ni concentrations in continental volcanic rocks. **(A)** A positive correlation between Ni vs. MgO in all volcanic rocks. **(B)** Variations of the Ni concentrations in komatiites. Histograms show the proportion of komatiite occurrences relative to all volcanic rocks in 250 Ma bins in our gridded dataset. The gray diamonds represent the Ni concentrations in individual komatiites. The blue circles are the mean values of Ni concentration in 200 Ma bins. All error bars are 2 standard errors of the means (s.e.m.). **(C)** A negative correlation between Ni vs. SiO_2 in non-komatiite (MgO <18 wt%) volcanic rocks. The bin size is 1 wt%. **(D)** Variations of mean Ni concentrations in basalts-andesites (green curve) and dacites-rhyolites (red curve) through time, respectively. The green and pink bands are 2 s.e.m. (For interpretation of the colors in the figure(s), the reader is referred to the web version of this article.)

tiating the oceanic Ni depletion at the Archean-Proterozoic boundary. Moreover, we demonstrate that from the Paleoproterozoic to the modern, seawater Ni concentrations have remained relatively stable, implying decreasing temperature but increasing pressure of mantle melting.

2. Methods

2.1. Data compilation and filtering

The freely accessible EarthChem rock database has synthesized the geochemical data from several other databases including GEOROC, PetDB, SedDB, NAVDAT, USGS, etc. In this study, we downloaded all available geochemical data for volcanic rocks sourced from GEOROC re-compiled by EarthChem Database (http://portal.earthchem.org/, accessed on 17 January 2020), including volcanic rocks spanning from ~3.5 Ga to the present (Supplementary Fig. 1), effectively representing the geological history of the Earth. As samples with ages of 2.4 to 2.2 Ga are limited in the database, we complemented the geochemical data with analyses of volcanic rocks formed during this period from several published papers (French and Heaman, 2010; Kumar et al., 2012; Nilsson et al., 2013; Stepanova et al., 2015). The data structure includes the literature reference, longitude and latitude, whole-rock composition, rock type, and age of each sample. We excluded samples that lacked ages or SiO_2 and MgO contents. Samples with SiO_2 contents greater than 80 wt% or less than 43 wt% were omitted as they are rarely seen, and might have been oversampled due to their scarcity. The data include rock samples that were collected from different continents and magmatic arcs around the world (Supplementary Fig. 2). Samples from the modern oceanic floor (e.g., mid-ocean ridge, oceanic islands, oceanic crust, etc.) were removed because the old oceanic volcanic rocks have been largely subducted. We also excluded kimberlites and carbonatites from the dataset because those rocks might have been oversampled due to their scarcity and special geochemical characteristics. The age uncertainty was restricted to be <100 Ma for Precambrian rocks and <50 Ma for Phanerozoic rocks to ensure the accuracy of our results. A final dataset containing whole-rock geochemical data for 96,317 volcanic rocks was prepared for the statistical analysis (Supplementary Dataset 1). In addition to the geochemical data of igneous rocks, we also include an updated BIF database of Ni concentrations in BIF (n=2,037; Supplementary Dataset 2) and a previously published shale database (Greber et al., 2017) (n=397; Supplementary Dataset 3).

2.2. Ni vs. SiO_2 and Ni vs. MgO

We divided the dataset into three groups based on age: Archean, Proterozoic, and Phanerozoic. The means and standard errors of the means of Ni concentrations were calculated for rocks with different SiO_2 and MgO contents. The bin size is 1 wt% of

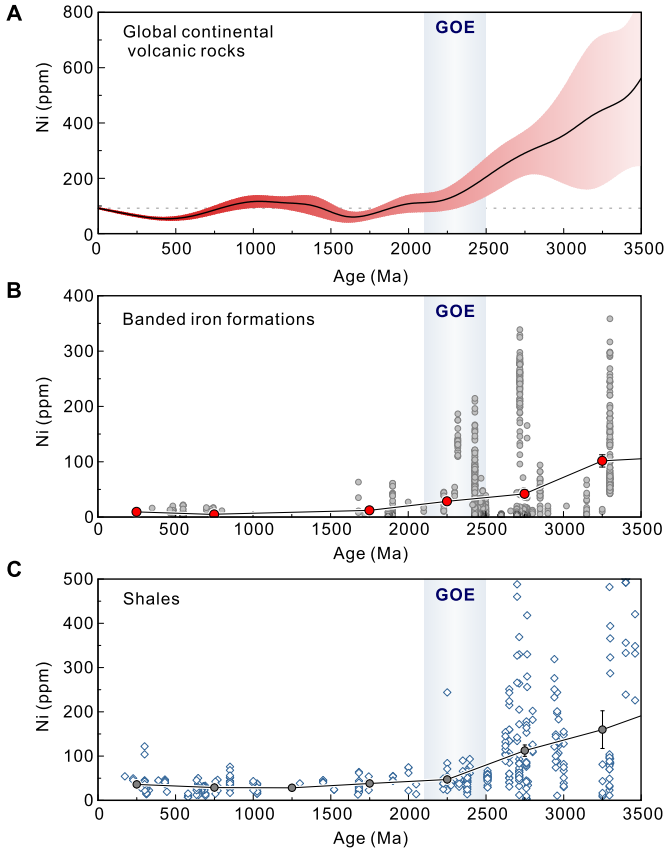

Fig. 2. Temporal trend of Ni concentrations in continental volcanic rocks compared to other proxies of oceanic Ni. (A) Temporal variation of Ni concentration in continental volcanic rocks. The black curve represents the mean values of Ni concentrations, while the red band denotes 2 s.e.m. We calculated the mean and 2 s.e.m. for each 200 Ma bin and connected the values using B-spline smoothing. **(B)** Ni concentrations in banded iron formations (2,037 samples). The gray circles show the Ni concentrations of individual analyses. Data are updated from Konhauser et al. (2015). The red-filled circles are mean values for 500 Ma bins. Error bars are 2 s.e.m. **(C)** Ni concentrations in shales (397 samples). The blue diamonds are the Ni concentrations of individual shale samples. The gray circles represent the mean values for 500 Ma bins. Error bars are 2 s.e.m. Data are from Greber et al. (2017). The light gray columns denote the Great Oxidation Event (2.5-2.1 Ga).

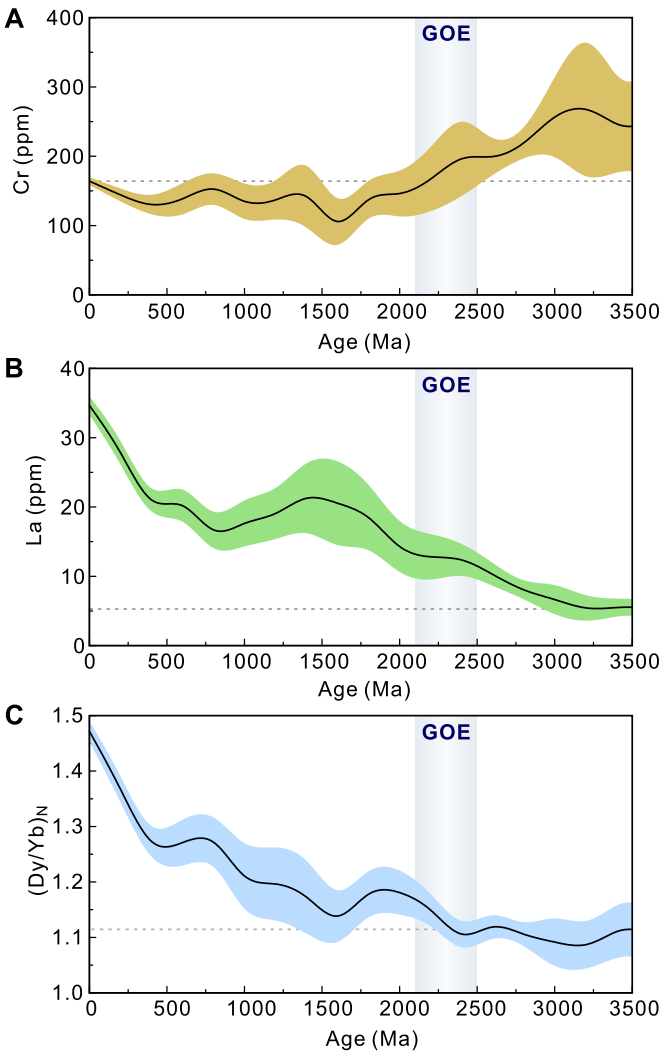

Fig. 3. Temporal variations of compatible, incompatible elements, and Dy/Yb in basalts-andesites. (A-C) The temporal trend of Cr, La, and chondrite-normalized (McDonough and Sun, 1995) Dy/Yb in basalts-andesite, respectively. The black curves show the mean values, while the color bands are 2 s.e.m. The light gray columns denote the Great Oxidation Event (2.5-2.1 Ga).

SiO_2 or MgO. A moving window of 2 wt% is applied to smooth the trend. Note that komatiites were excluded in the plots of Ni vs. SiO_2 as we treat komatiites separately.

2.3. Secular trend of Ni concentration

We performed the outlier elimination for the dataset before the statistical analysis by trimming 0.2% of the data to exclude anomalous data for the whole dataset. As the range of Ni concentrations varied considerably in rocks of different ages, we also eliminated outliers (i.e., keeping the data bounded by the 5th and 95th percentiles) for every 200 Ma age bin. The secular variations of Ni concentrations in global continental volcanic rocks through time were estimated using a grid-resampling method because the rock samples in the dataset were not evenly sampled at different locations. For instance, there are tens of samples in certain areas but only sporadic samples in others. Particularly, Archean komatiites were often over-sampled at outcrops compared to dacites or rhyolites. Thus, we developed a longitude-latitude-age griding method to diminish the spatially unbalanced sampling effect. We rounded the longitude and latitude coordinates of each sample to the nearest integral degree and rounded the age of each sample to the nearest 10 Myr (million years) so that all the rocks were re-located to a 1°×1°×10 Ma grid. We then calculated average Ni concentrations in rocks at each node with the same rounded coordinates and ages in MATLAB®. After this step, a gridded resampled dataset was obtained. A comparison between the original dataset and the gridded dataset is shown in Supplementary Fig. 3.

The mean Ni concentrations in volcanic rocks through time were calculated in MATLAB®, along with the standard error of the mean for every 200 Ma age bin using the Bootstrap method with 10,000 iterations of resampling. Rocks older than 3500 Ma were excluded from this resampling calculation due to the very limited number of samples. Similarly, komatiites after the Paleoproterozoic were excluded because they are rare and may have been oversampled. The secular trend of Ni concentrations in volcanic rocks was created by connecting the mean values and 2 standard errors of the means (s.e.m.) of all the bins using the B-spline smoothing method. To understand the variation of Ni concentrations in different types of volcanic rocks, we also created the temporal trends in Ni for the komatiite (MgO≥18 wt%), basalts-andesites (SiO_2 = 45-63 wt%, MgO<18 wt%), and dacite-rhyolite (SiO_2 = 63-80 wt%, MgO<18 wt%) groups. Following these methods, the secular variation of Ni concentrations in BIF and shales were also calculated in order to facilitate a direct comparison.

3. Results

The compositional trends of Ni vs. MgO for global-scale volcanic rocks show identical positive correlations between Ni and MgO contents amongst the Archean, Proterozoic, and Phanerozoic age groups (Fig. 1A). A distinct feature of Archean rocks is that the MgO contents reach as high as 30 wt%, whereas the Proterozoic and Phanerozoic rocks with >18 wt% MgO are scarce and insufficient for plotting. This trend correlated with the fact that the eruption of komatiites mainly occurred during the Archean, with some in the early Paleoproterozoic, and only occasional appearances in the Neoproterozoic and Phanerozoic (Condie et al., 2016; Condie and O'Neill, 2010; Hanski et al., 2004; Kamenetsky et al., 2010; Zhang, 1997) (Fig. 1B). In terms of Archean komatiites (>18 wt% MgO), the average Ni concentration at ~3.5 Ga was ~1,900 ppm and gradually decreased to ~900 ppm at ~2.5 Ga (Fig. 1B). At ~2.0 Ga, the average Ni concentration in komatiites rebounded to a level of ~1,370 ppm, approximately equal to the value at 3.0-2.5 Ga but remained systematically lower than in older (>3.0 Ga) komatiites. The Neoproterozoic and Phanerozoic komatiites contain ~850-100 ppm Ni on average.

In the compositional trends of Ni vs. SiO_2 in non-komatiite (MgO <18 wt%) volcanic rocks (Fig. 1C), we observe that the basaltic-andesitic rocks (SiO_2 = 45-63 wt%, hereafter referred to as basalts-andesites) formed in the Archean contain systematically higher Ni concentrations than Proterozoic and Phanerozoic basalts-andesites. A temporal change in average Ni concentrations of basalts-andesites shows a descending trend from ~150 ppm at 3.5 Ga to ~80 ppm at 2.0 Ga (Fig. 1D), approximately equal to modern values. After 2.0 Ga, the Ni concentrations oscillated within a narrow range of ~60 to ~90 ppm (Fig. 1D). By contrast, dacitic-rhyolitic rocks (SiO_2 = 63-80 wt%, hereafter referred to as dacites-rhyolites) are characterized by similar Ni concentrations across each of the geological eras (Fig. 1C), from peak concentrations of ~25 ppm at 3.5 Ga, and then gradually decreasing to ~12 ppm at 2.0 Ga (Fig. 1D). Thereafter, the average Ni concentration in dacites-rhyolites became relatively constant with minor fluctuations, reaching a modern value of ~13 ppm.

In the secular trend of Ni in global continental volcanic rocks (Fig. 2A), the average concentration exhibits a dramatic drop from ~500 to ~200 ppm during the Archean. A relatively large uncertainty is observed for the period between 3.5 and 2.8 Ga, the result of a large standard deviation of the data. It is noteworthy that the average Ni concentrations after the GOE had been reduced to a level in proximity to the modern value of ~90 ppm (Fig. 2A). In other words, the average Ni concentration in continental volcanic rocks has been relatively constant from ~2.0 Ga to the present.

The average Ni concentrations in both BIF and shales show a decline during the Archean (Figs. 2B and 2C). From 3.5 to 2.0 Ga, the mean value of Ni concentrations in BIF gradually decreased from ~100 to ~12 ppm (Fig. 2B), while the mean Ni concentration in shales dropped from ~160 to ~38 ppm (Fig. 2C). Similar to the volcanic rocks, both the BIF and shale records show relatively constant Ni concentrations from ~2.0 Ga to the present.

4. Discussion

4.1. Decreasing Ni in Archean volcanic rocks

The most striking result of our statistical analyses is that the average Ni concentrations of global continental volcanic rocks were very high in the early Archean and gradually decreased until the GOE (Fig. 2A). This can be predominantly attributed to the gradually reduced proportion of komatiites relative to all volcanic rocks from ~25% in the Paleoarchean to ~2% in the Paleoproterozoic (Fig. 1B). Moreover, our statistical analyses indicate that the average Ni concentrations in komatiites progressively decreased during the Archean (Fig. 1B). This may have compounded the decline in Ni originally observed in BIF (Konhauser et al., 2009). In addition to the changes in komatiites, we observe that the basalts-andesites rocks also supplied Ni, albeit at lesser amounts than komatiites. Nickel abundance in basalts-andesites is systematically higher in the Archean compared to the Proterozoic and Phanerozoic (Figs. 1C and 1D). On the other hand, the Ni concentrations in dacites-rhyolites did not change substantially over time (Figs. 1C and 1D). Since the proportion of basalts-andesites and dacites-rhyolites have been generally stable throughout Earth's history (Keller and Harrison, 2020), it appears that dacites-rhyolites would unlikely have affected the secular evolution of the total volcanic Ni supply to the oceans. As such, we conclude that the decreasing trend of average Ni concentrations in the bulk volcanic rocks before the GOE (Fig. 2A) was caused by the integrated effect of the gradually reduced proportion of komatiites and the decline of Ni concentrations in komatiites and basalts-andesites (Figs. 1B and 1D).

Nickel is a compatible element that is strongly partitioned into sulfide and olivine during the melting of mantle peridotites (McDonough and Sun, 1995; Pedersen, 1979; Rajamani and Naldrett, 1978). Consequently, the Ni concentration in basalts-andesites is a potential indicator for tracking the temperature of melting (Keller and Schoene, 2018, 2012). In this regard, the declining trends of Ni concentrations in basalts-andesites (Fig. 1D) over the Archean and early Paleoproterozoic may reflect the decreasing temperature of magma generation, which, in turn, was most likely caused by secular mantle cooling (Herzberg et al., 2010; Keller and Schoene, 2012). We also plotted the temporal variations of Cr and La concentrations in basalts-andesites to validate the Ni trend (Figs. 3A and 3B). The results exhibit a descending trend of Cr and an ascending trend of La before ~2.0 Ga. Because Cr is a compatible element while La is an incompatible element during the melting of mantle peridotite (Green and Pearson, 1983; Nielsen et al., 1992; Villemant, 1988), the opposite trends of Cr and La from 3.5 to 2.0 Ga further demonstrate the gradually reduced degree of melting, attributed to the secular cooling of the upper mantle.

Although magma differentiation could also affect the concentrations of compatible and incompatible elements in basalts-andesites, it has been suggested that the formation of volcanic rocks with specific silica content should have undergone similar degrees of differentiation regardless of age (Keller and Schoene, 2018). Given that the relative frequency of volcanic rocks with different silica contents has changed little over geological time (Keller and Harrison, 2020), we conclude that the differentiation is unlikely to have resulted in a systematic increase or decrease in the average Ni concentrations of basalts-andesites. Crustal contamination, hydrothermal alteration, and metasomatism may have also influenced the concentrations of trace elements in these volcanic rocks. However, it has been suggested that such effects on igneous rocks are nearly invariant over the past 3.5 Ga and should not generate secular changes in element concentrations (Keller and Schoene, 2018).

4.2. Decreasing Ni in Archean oceans

The supply of Ni from land to the oceans would have occurred in both dissolved ionic form and as suspended sediment, with the Ni subsequently being incorporated into either BIF or shales, respectively. The former are chemical sediments that precipitated out of seawater, capturing dissolved ions in a predictable manner based on the surface reactivity of the primary iron sediment, comprised of Fe(III) oxyhydroxides (Konhauser et al., 2017; Robbins et al., 2016). As shown in an updated database here, the BIF record displays a significant decline in average Ni concentrations

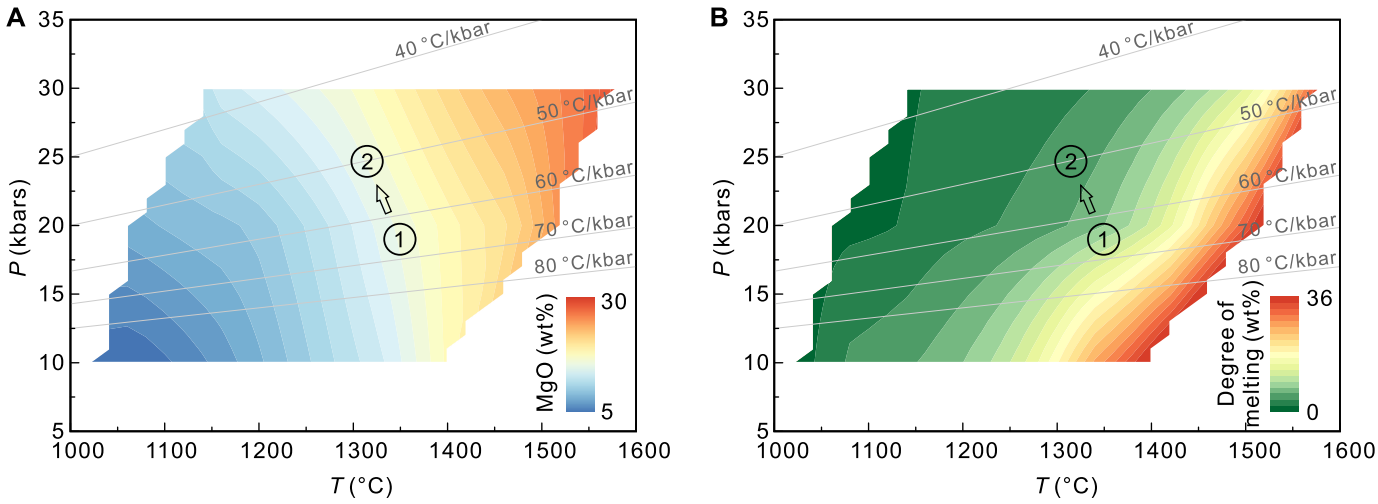

Fig. 4. Comparison between the MgO content in the melt and the degree of partial melting. A series of isobaric batch melting models was performed in pMELTS. The composition of the source is the primitive mantle (McDonough and Sun, 1995) with 0.2 wt% H_2O. **(A)** The relation between the MgO contents in the melts and the *P-T* conditions of melting. **(B)** Relation between the degree of melting and the P-T condition. The numbers 1 and 2 within black circles denote Condition 1 and Condition 2, respectively. The gray lines with labels show the conductive geotherm. Note that the geotherms in the adiabatic mantle are not shown.

from 3.5 to 2.5 Ga (Fig. 2B). Such a declining trend in Ni abundances is also recorded in shales (Fig. 2C) and sedimentary pyrite (Large et al., 2014). Interestingly, it is apparent that the secular trend of average Ni concentrations in global continental volcanic rocks (Fig. 2A) is quite similar to the evolution of Ni in BIF and shales (Fig. 2B and 2C). This suggests a causal relationship in that the gradually decreasing Ni in continental volcanic rocks leads to diminishing dissolved and clastic Ni fluxes from the continent to the ocean, which in turn, was manifest by an irreversible decline in the dissolved Ni concentration of Archean seawater. Even if extrapolated oceanic Ni concentrations based on the molar Ni/Fe ratios in BIF (Konhauser et al., 2009) were overestimated or underestimated (Eickhoff et al., 2014), the hypothesized drop in dissolved Ni concentration during the late Archean is validated by the temporal variation in the average Ni concentrations of continental volcanic rocks. As originally proposed by Konhauser et al. (2009), the implications of declining Ni supply to the oceans would have been the progressive starvation of the marine microorganisms that needed it the most, that being the methanogens. Then, as methanogenic activity waned, their former environments would have become occupied by other microorganisms, such as cyanobacteria in the littoral zone (Eigenbrode and Freeman, 2006) and sulfate reducing bacteria in the deeper water column and surface sediments (Zahnle et al., 2006). Indeed, our new data verifying that a decline in the volcanic sourcing of Ni to the oceans supports the concept of a "bioinorganic bridge" (Anbar and Knoll, 2002), whereby an Archaea's enzymatic reliance on an increasingly scarce supply of Ni links changes in mantle evolution with the redox state of the atmosphere.

We note that, in this study, we only focused on volcanic rocks because they undergo weathering and erosion immediately after their eruption. Although the terrestrial Ni supply was also sourced from exposed plutonic and sedimentary rocks, we propose that the compositional variation of plutonic and sedimentary rocks should not significantly influence the bulk Ni flux to the ocean because most of those rocks do not contain Ni with abundances as high as komatiite, except the rare ultramafic intrusions with Ni enrichment or mineralization. Given the consistency of the Ni trend between the volcanic and marine sedimentary rocks (BIF and shales), we conclude that the decreasing Ni concentrations in continental volcanic rocks would have independently resulted in diminishing clastic and dissolved Ni fluxes to the ocean before the GOE.

4.3. The stabilization of Ni after the GOE

Although the decline of dissolved Ni in the Archean ocean can be reasonably linked with the secular cooling of the mantle, the constancy of the Ni concentrations in volcanic and marine sedimentary rocks after the GOE (Fig. 2) requires further explanation. As komatiites had largely disappeared after ~2.0 Ga (Fig. 1B), the bulk volcanic Ni flux to the oceans thereafter was predominantly controlled by the Ni concentration in basalts-andesites. However, if the increasing trend of La concentrations in basalts-andesites (Fig. 3B) is consistent with the progressively lowering degree of partial melting and the secular cooling of the mantle throughout Earth's history (Keller and Schoene, 2018), the absence of a continuous decline in concentrations of Ni (and Cr) in basalts-andesites after ~2.0 Ga (Figs. 1D and 3A) may seem to contradict the thermal evolution of the mantle and the temporal variation of La (Fig. 3B). Yet, no inconsistency needs to exist here because the concentrations of compatibles elements in basaltic magma may also be affected by the pressure of melting.

To assess the temporal changes in the pressure of mantle melting, we plotted the average Dy/Yb in basalts-andesites through time. The Dy/Yb in basaltic melts may be an effective proxy that reflects melting pressures due to the similar incompatibility of Dy-Yb and a higher Yb partitioning coefficient in the residual garnets, which are more stable at higher pressure (McKenzie and O'Nions, 1991; Tang et al., 2019). As expected, the Dy/Yb rapidly increases from ~2.0 Ga to the present, suggesting a concomitant increase in melting pressure (Fig. 3C). To elucidate the effect of pressure on compatible elements during mantle melting, we performed a pMELTS simulation for an isobaric equilibrium batch melting model of mantle peridotite with an initial composition representative of the primitive mantle (McDonough and Sun, 1995) with 0.2 wt% H_2O over the pressure of 10-30 kbar and temperatures of 1000-1600 °C. Given the positive correlation between Ni and MgO in volcanic rocks (Fig. 1A), we created a series of MgO isolines on a *P-T* (pressure-temperature) diagram (Fig. 4A) that reflect the behavior of MgO (and therefore Ni) during equilibrium melting. The diagram reveals that the MgO content in the melt will decrease if the temperature decreases but will increase if the pressure increases (Fig. 4A). By contrast, the degree of partial melting decreases with the decreasing temperature and increasing pressure (Fig. 4B), distinct from the behavior of MgO. Based on these findings, we propose that the increasing pressure of melting af-

ter ~2.0 Ga (Fig. 3C) might have counterbalanced the effect of the decreasing temperature of melting on the compatible elements (e.g., Ni and Cr) in basalts-andesites so that their concentrations remained effectively static (Figs. 1D and 3A). The primary driver of the increasing melting pressure is the secular cooling of the mantle. Abundant models have shown that the cooling of the mantle should result in a lower continental conductive geotherm (dT/dP) (Burke and Kidd, 1978; Strong and Stevens, 1974). Here we use a schematic model to show the variation of the P-T condition of mantle melting over time. Assuming that magma equilibration sometime in the Proterozoic occurred at Condition 1 (see Fig. 4A), the secular cooling of the mantle might lead to a drop of the conductive geotherm (dT/dP) so that magma equilibration sometime in the Phanerozoic occurred at Condition 2. During this process, the MgO content in the melt is generally constant with the decreasing temperature and increasing pressure of melting. This hypothesis explains the general constancy of the dissolved Ni concentrations in the ocean (Fig. 2B) and the particulate Ni concentrations in terrigenous sedimentary rocks (Fig. 2C) following the GOE.

5. Conclusions

We show that the average Ni concentrations in global continental volcanic rocks rapidly decreased during the Archean and early Paleoproterozoic, stabilizing at a near-constant level after the GOE. This view is consistent with the evolution of the oceanic Ni reservoir as recorded by both BIF and shales. This trend lends credence to the hypothesis that the diminishing supply of continentally sourced volcanic Ni to the oceans before the GOE - due to the secular cooling of the mantle - resulted in a decline towards oceanic Ni concentrations of near modern levels. The decrease of dissolved Ni concentration in the Archean would have marginalized methanogens and significantly depressed the biogenic methane production, which eventually facilitated the irreversible oxygenation of the atmosphere. After ~2.0 Ga, relatively stable Ni concentrations in the oceans were maintained by the general constancy of Ni concentration in basalts-andesites, which in itself was a consequence of the balanced effect of decreasing temperature and increasing pressure during mantle melting.

CRediT authorship contribution statement

H.L. and K.O.K. conceived this research. H.L. processed the igneous data. K.O.K. and L.J.R. compiled the BIF data. H.L., K.O.K., and L.J.R. wrote the paper. W.D.S contributed to the scientific presentation. All authors participated in the discussions.

Declaration of competing interest

The authors declare that they have no known competing financial interests or personal relationships that could have appeared to influence the work reported in this paper.

Data and code availability

The datasets and computer code are available at https://github.com/CodrIocas/Nickel.git.

Acknowledgements

The authors thank Ryan McKenzie and an anonymous reviewer for comments that greatly improved the manuscript. This study was supported by the Strategic Priority Research Program of the Chinese Academy of Sciences (XDB18020102), the National Key R & D Program of China (2016YFC0600408), and the National Natural Science Foundation of China (42073011). K.O.K. (RGPIN–165831) and L.J.R. (RGPIN-2021-02523) gratefully acknowledge the support of Natural Sciences and Engineering Research Council of Canada (NSERC) Discovery grants.

Appendix A. Supplementary material

Supplementary material related to this article can be found online at https://doi.org/10.1016/j.epsl.2021.117116.

References

Anbar, A.D., Knoll, A.H., 2002. Proterozoic ocean chemistry and evolution: a bioinorganic bridge? Science 297, 1137.
Burke, K., Kidd, W., 1978. Were Archean continental geothermal gradients much steeper than those of today? Nature 272, 240.
Canfield, D.E., Habicht, K.S., Thamdrup, B., 2000. The Archean sulfur cycle and the early history of atmospheric oxygen. Science 288, 658–661.
Catling, D.C., Zahnle, K.J., McKay, C.P., 2001. Biogenic methane, hydrogen escape, and the irreversible oxidation of early Earth. Science 293, 839.
Condie, K.C., Aster, R.C., van Hunen, J., 2016. A great thermal divergence in the mantle beginning 2.5 Ga: geochemical constraints from greenstone basalts and komatiites. Geosci. Front. 7, 543–553.
Condie, K.C., O'Neill, C., 2010. The Archean-Proterozoic boundary: 500 My of tectonic transition in Erath history. Am. J. Sci. 310, 775–790.
Eickhoff, M., Obst, M., Schröder, C., Hitchcock, A., Tyliszczak, T., Martinez, R.E., Robbins, L.J., Konhauser, K.O., Kappler, A., 2014. Nickel partitioning in biogenic and abiogenic ferrihydrite: the influence of silica and implications for ancient environments. Geochim. Cosmochim. Acta 140, 65–79.
Eigenbrode, J.L., Freeman, K.H., 2006. Late Archean rise of aerobic microbial ecosystems. Proc. Natl. Acad. Sci. 103, 15759.
French, J.E., Heaman, L.M., 2010. Precise U–Pb dating of Paleoproterozoic mafic dyke swarms of the Dharwar craton, India: Implications for the existence of the Neoarchean supercraton Sclavia. Precambrian Res. 183, 416–441.
Greber, N.D., Dauphas, N., Bekker, A., Ptacek, M.P., Bindeman, I.N., Hofmann, A., 2017. Titanium isotopic evidence for felsic crust and plate tectonics 3.5 billion years ago. Science 357, 1271–1274.
Green, T.H., Pearson, N.J., 1983. Effect of pressure on rare Earth element partition coefficients in common magmas. Nature 305, 414–416.
Habicht, K.S., Gade, M., Thamdrup, B., Berg, P., Canfield, D.E., 2002. Calibration of sulfate levels in the Archean ocean. Science 298, 2372.
Hanski, E., Walker, R.J., Huhma, H., Polyakov, G.V., Balykin, P.A., Tran Trong, H., Ngo Thi, P., 2004. Origin of the Permian-Triassic komatiites northwestern Vietnam. Contrib. Mineral. Petrol. 147, 453–469.
Haqq-Misra, J.D., Domagal-Goldman, S.D., Kasting, P.J., Kasting, J.F., 2008. A revised, hazy methane greenhouse for the Archean Earth. Astrobiology 8, 1127–1137.
Herzberg, C., Condie, K., Korenaga, J., 2010. Thermal history of the Earth and its petrological expression. Earth Planet. Sci. Lett. 292, 79–88.
Kamenetsky, V.S., Gurenko, A.A., Kerr, A.C., 2010. Composition and temperature of komatiite melts from Gorgona Island, Colombia, constrained from olivine-hosted melt inclusions. Geology 38, 1003–1006.
Keller, B., Schoene, B., 2018. Plate tectonics and continental basaltic geochemistry throughout Earth history. Earth Planet. Sci. Lett. 481, 290–304.
Keller, C.B., Harrison, T.M., 2020. Constraining crustal silica on ancient Earth. Proc. Natl. Acad. Sci. USA 117, 21101–21107.
Keller, C.B., Schoene, B., 2012. Statistical geochemistry reveals disruption in secular lithospheric evolution about 2.5 Gyr ago. Nature 485, 490–493.
Konhauser, K.O., Pecoits, E., Lalonde, S.V., Papineau, D., Nisbet, E.G., Barley, M.E., Arndt, N.T., Zahnle, K., Kamber, B.S., 2009. Oceanic nickel depletion and a methanogen famine before the great oxidation event. Nature 458, 750–753.
Konhauser, K.O., Planavsky, N.J., Hardisty, D.S., Robbins, L.J., Warchola, T.J., Haugaard, R., Lalonde, S.V., Partin, C.A., Oonk, P.B.H., Tsikos, H., Lyons, T.W., Bekker, A., Johnson, C.M., 2017. Iron formations: a global record of Neoarchaean to Palaeoproterozoic environmental history. Earth-Sci. Rev. 172, 140–177.
Konhauser, K.O., Robbins, L.J., Pecoits, E., Peacock, C., Kappler, A., Lalonde, S.V., 2015. The Archean nickel famine revisited. Astrobiology 15, 804–815.
Kumar, A., Hamilton, M.A., Halls, H.C., 2012. A Paleoproterozoic giant radiating dyke swarm in the Dharwar Craton, southern India. Geochem. Geophys. Geosyst. 13.
Large, R.R., Halpin, J.A., Danyushevsky, L.V., Maslennikov, V.V., Bull, S.W., Long, J.A., Gregory, D.D., Lounejeva, E., Lyons, T.W., Sack, P.J., McGoldrick, P.J., Calver, C.R., 2014. Trace element content of sedimentary pyrite as a new proxy for deep-time ocean–atmosphere evolution. Earth Planet. Sci. Lett. 389, 209–220.
Lyons, T.W., Reinhard, C.T., Planavsky, N.J., 2014. The rise of oxygen in Earth's early ocean and atmosphere. Nature 506, 307–315.
McDonough, W.F., Sun, S.S., 1995. The composition of the Earth. Chem. Geol. 120, 223–253.
McKenzie, D.A.N., O'Nions, R.K., 1991. Partial melt distributions from inversion of rare Earth element concentrations. J. Petrol. 32, 1021–1091.

Nielsen, R.L., Gallahan, W.E., Newberger, F., 1992. Experimentally determined mineral-melt partition coefficients for Sc, Y and REE for olivine, orthopyroxene, pigeonite, magnetite and ilmenite. Contrib. Mineral. Petrol. 110, 488–499.

Nilsson, M.K.M., Klausen, M.B., Söderlund, U., Ernst, R.E., 2013. Precise U–Pb ages and geochemistry of Palaeoproterozoic mafic dykes from southern West Greenland: linking the North Atlantic and the Dharwar cratons. Lithos 174, 255–270.

Pavlov, A.A., Kasting, J.F., Brown, L.L., Rages, K.A., Freedman, R., 2000. Greenhouse warming by CH4 in the atmosphere of early Earth. J. Geophys. Res., Planets 105, 11981–11990.

Pedersen, A.K., 1979. Basaltic glass with high-temperature equilibrated immiscible sulphide bodies with native iron from disko, central West Greenland. Contrib. Mineral. Petrol. 69, 397–407.

Poulton, S.W., Bekker, A., Cumming, V.M., Zerkle, A.L., Canfield, D.E., Johnston, D.T., 2021. A 200-million-year delay in permanent atmospheric oxygenation. Nature 592, 232–236.

Rajamani, V., Naldrett, A.J., 1978. Partitioning of Fe, Co, Ni, and Cu between sulfide liquid and basaltic melts and composition of Ni-Cu sulfide deposits. Econ. Geol. 73, 82–93.

Robbins, L.J., Lalonde, S.V., Planavsky, N.J., Partin, C.A., Reinhard, C.T., Kendall, B., Scott, C., Hardisty, D.S., Gill, B.C., Alessi, D.S., Dupont, C.L., Saito, M.A., Crowe, S.A., Poulton, S.W., Bekker, A., Lyons, T.W., Konhauser, K.O., 2016. Trace elements at the intersection of marine biological and geochemical evolution. Earth-Sci. Rev. 163, 323–348.

Stepanova, A.V., Salnikova, E.B., Samsonov, A.V., Egorova, S.V., Larionova, Y.O., Stepanov, V.S., 2015. The 2.31Ga mafic dykes in the Karelian Craton, eastern Fennoscandian shield: U–Pb age, source characteristics and implications for continental break-up processes. Precambrian Res. 259, 43–57.

Strong, D.F., Stevens, R.K., 1974. Possible thermal explanation of contrasting Archean and Proterozoic geological regimes. Nature 249, 545–546.

Tang, M., Lee, C.-T.A., Chen, K., Erdman, M., Costin, G., Jiang, H., 2019. Nb/Ta systematics in arc magma differentiation and the role of arclogites in continent formation. Nat. Commun. 10, 235.

Villemant, B., 1988. Trace element evolution in the Phlegrean Fields (Central Italy): fractional crystallization and selective enrichment. Contrib. Mineral. Petrol. 98, 169–183.

Zahnle, K., Claire, M., Catling, D., 2006. The loss of mass-independent fractionation in sulfur due to a Palaeoproterozoic collapse of atmospheric methane. Geobiology 4, 271–283.

Zhang, Z.-J., 1997. Geochemical characteristics of basic and ultrabasic metavolcanics from the Proterozoic Kuanping Group in the Qinling orogenic belt, China: petrogenetic and tectonic implications. J. Mineral. Pet. Econ. Geol. 92, 25–40.